

Swash Zone Morphodynamics and Sediment Transport Processes

K. Todd Holland¹, Asbury H. Sallenger, Jr.², Britt Raubenheimer³, and Steve Elgar³

Abstract

Observations of foreshore morphologic change and swash flow velocities were made at Duck, NC in an effort to estimate cross-shore sediment flux magnitudes. The three-dimensional foreshore surface over an approximately 10 x 20m study area was determined repeatedly to roughly centimeter accuracy using a stereometric video method. Sediment flux magnitudes derived from the temporal gradient of these data showed erosion rates of over 25 cm/hr. Near-bed, cross-shore swash velocities were measured at multiple cross-shore locations using a separate video technique. Swash velocities estimated using this method were found to be consistent with current measurements obtained using acoustic Doppler and ducted impeller current meters. The swash zone profile observations and velocity estimates were used to test an energetics-based total load sediment transport model. Although the trends of both the model and the observations were qualitatively consistent, the magnitudes and positioning of observed sediment fluxes did not match the transport model predictions. This discrepancy implies that other factors, such as water depth variations, infiltration, or sediment advection, may be important.

Introduction

It is generally recognized that gradients of sediment flux across the swash zone contribute significantly to beach morphological change. However, the present understanding of sediment transport mechanisms in this region is poor, partially owing to the complexity of foreshore processes. Nonlinearity and feedback between forcing and response are common. Yet even more problematic is the fact that measurements of fluid motions and sediment concentrations are difficult to obtain in this dynamic region. Swash flows move in a Lagrangian sense requiring either very dense arrays of in-situ sensors, dual-resistance runup wires (Guza and Thornton 1982; Raubenheimer et al. 1995), or

¹Naval Research Laboratory, Code 7442, Stennis Space Center, MS 39529-5004

²USGS Center for Coastal Geology, 600 4th St. S, St. Petersburg, FL 33071

³Washington State University, EECS 2752, Pullman, WA 99164

remote sensing methods (Holland et al. 1995). In addition, the foreshore surface itself may change rapidly making estimation of the measurement elevation complicated.

In previous studies of swash zone morphology and associated sediment transport, coarsely sampled changes in bed elevation have been used to infer total load sediment transport rates (Duncan 1964; Howd and Holman 1987; Sallenger and Richmond 1984; Waddell 1976); and either optical sensors or traps have been used to monitor suspended and bedload concentrations (Beach and Sternberg 1992; Horn and Mason 1994; Osborne and Rooker 1997; and others). Although much is known about fluid motions in the swash zone and the above studies give glimpses of relative sediment concentration magnitudes, there is a great need for simultaneous measurement of hydrodynamic forcing and morphodynamic response to advance foreshore sediment transport modeling. This deficiency is even more pronounced with respect to relatively large temporal and spatial scales (hours to days and 10s to 100s of meters, respectively).

This paper presents new swash observations collected at Duck NC with a recently developed stereometric video system and a video-based current meter method that show great promise in overcoming the difficulties mentioned above. The observations of profile change and cross-shore swash velocity are used to develop and validate a simple model of swash zone sediment transport. The correlation between model estimates and observations is then discussed.

Study Site and Field Methods

Data were obtained at the US Army Corps of Engineers' Field Research Facility (FRF) at Duck, NC. Duck is multi-barred, intermediate to reflective beach with a tidal range of approximately 2 m. The foreshore slope is roughly 1:12. A large number of experiments have taken place at the FRF field site with many swash observations indicating infragravity dominated motions at the shoreline, especially during storms.

To quantify net sediment transport and morphologic change in the swash zone, foreshore surface measurements were made over a study region of dimensions 10 m in the cross-shore and 20 m in the alongshore during the DUCK94 experiment. Three-dimensional (3-D) foreshore topography was determined to roughly centimeter accuracy by using a stereometric video method (described fully in Holland and Holman 1997). By monitoring the progression of the swash line using edge detection algorithms, multiple views of the foreshore study area allow determination of point object positions (x,y,z) for each pixel along the swash edge. Repeating the process for each subsequent edge over the swash cycle results in several thousand estimates of the foreshore surface per wave. Although observations were made over a much larger time interval, the data presented in this paper were obtained during a particularly dynamic period of erosion on October 10, 1994. A burst sampling mode was employed to measure swash excursions and elevations over the foreshore region approximately once every 15 minutes at a rate of 6 Hz [Figure 1].

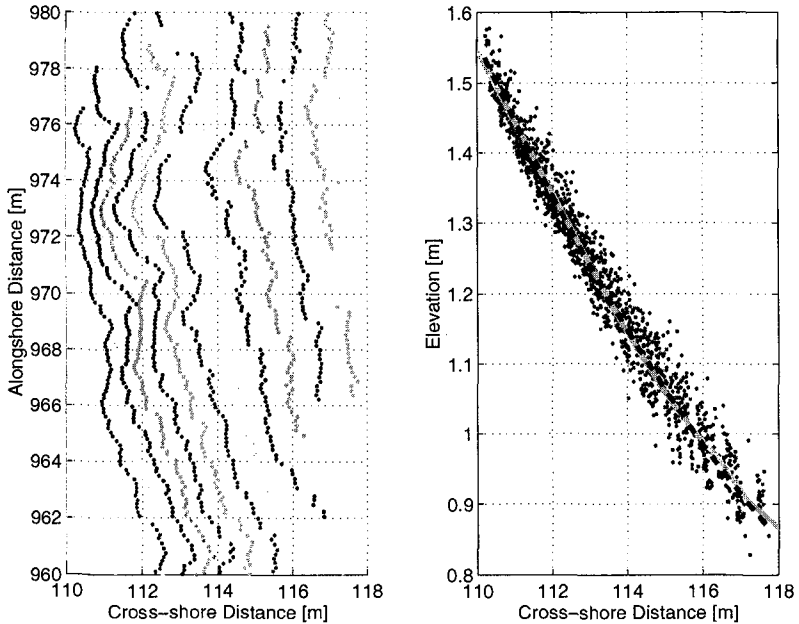


Figure 1: Left panel shows stereo-estimated swash edge positions intensity coded by time (temporal separation interval of 0.33 s). Right panel shows elevation versus cross-shore distance as determined by the stereo method (dots) and GPS surveying methods (dashed).

Optimal interpolation of the nearly 7000 stereo estimates (solid) yields a cross-shore profile with a root-mean-square deviation from the surveyed profile of 1.4 cm.

Corresponding cross-shore swash velocities were estimated using a new application of an existing video method known as a timestack (Holland et al. 1995). Since timestacks [Figure 2] represent the temporal variation in pixel intensity along a given cross-shore profile, Lagrangian estimates of the swash edge speed can be calculated as the time derivative of the measured cross-shore swash position. In contrast, Eulerian estimates of cross-shore currents, $u(x)$, were calculated at specific cross-shore distances using the edge speeds during uprush and backwash derived from timestacks (sampled at 10 Hz). In doing so we assumed that fluid particles immediately behind the bore front move at the speed of the bore and that a constant velocity gradient exists from the moment the swash bore reaches the video sensor till the time of maximum backwash. Velocities were set to zero for times during which the virtual sensor was dry. Using this method, saw-toothed, swash velocity time series were computed at eleven locations spaced by one meter along the cross-shore transect in the center of the study area. Figure 3 exemplifies the differences in velocities at two cross-shore positions.

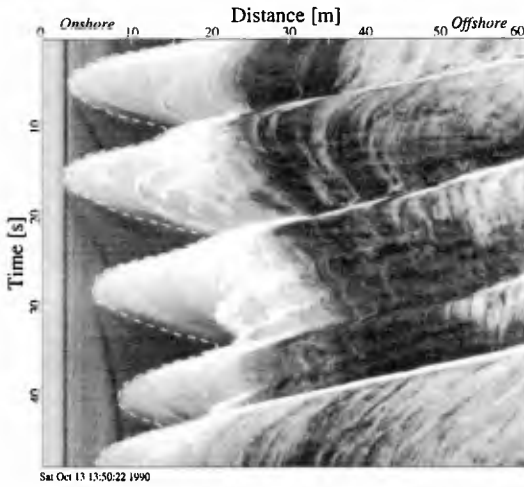


Figure 2: Video timestack showing swash edge position (dashed) as a function of time and cross-shore position (from Holland and Holman 1993).

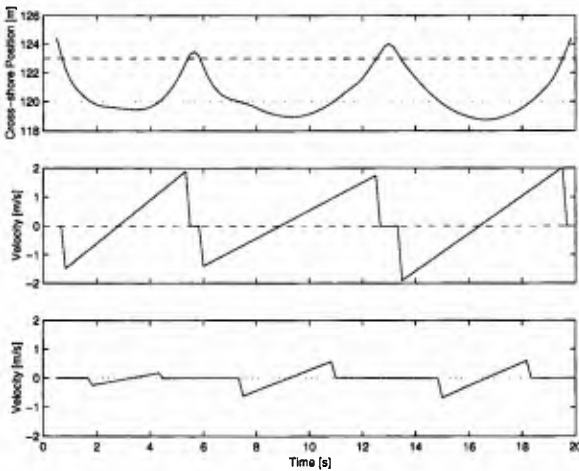


Figure 3: Schematic of video method for extracting cross-shore swash currents at two cross-shore ($x=123$ and $x=120$, middle and bottom respectively) locations from position time series (top). Position decreases landward and negative velocities correspond to onshore flow.

To determine the validity of this video method for deriving cross-shore currents in the swash zone, measurements made using this technique were compared to velocity measurements obtained using Acoustic Doppler Velocimeter (ADV) and ducted impeller current meters. During the SANDYDUCK experiment, horizontal and vertical swash velocities approximately 5 cm above the bed were measured at a 2 Hz sampling rate at one location using a Sontek ADV [Figure 4]. Additionally, 4-Hz cross-shore current measurements at 4 and 8 cm above the beach surface were available from "Smith" ducted impeller sensors deployed during an experiment at Gleneden OR in 1994 (Puleo et al. submitted). Figure 5 shows an example of the comparison. In general, the results are similar. The timing of the uprushes measured by the in-situ gauges closely corresponds to that of the leading edge of the swash as it reaches the sensor location. Current meter velocities were also very small during time intervals where the video indicated the sensor was dry ($u = 0$ m/s). Peak uprush and backwash velocity magnitudes were often similar and the slopes of the temporal velocity gradients from each method were roughly equivalent. Since there was only a small amount of structure in the interval between the beginning of uprush and the end of backwash, the constant gradient assumption in the video method appears justified.

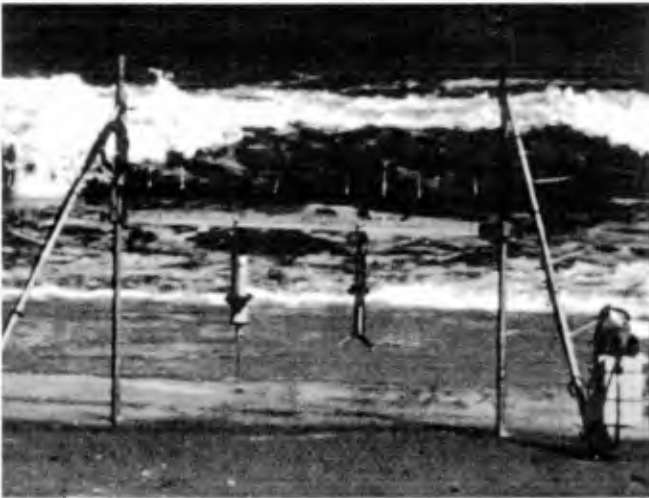


Figure 4: ADV instrumentation designed to monitor swash velocities as part of the SANDYDUCK experiment.

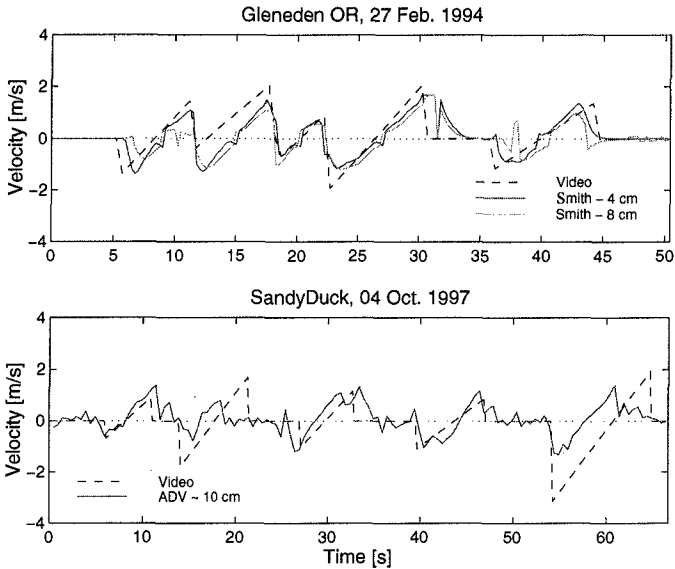


Figure 5: Time series showing cross-shore current estimates in swash zone obtained using video and in-situ instrumentation.

Table 1 shows the quantitative results of the comparison of 333 swash events. The means of the various parameters are comparable, although video-based uprush and backwash speeds and swash durations were on average of greater magnitude than the observations from the in-situ instrumentation. Estimates of higher moments of cross-shore currents (e.g. u^3) were quite variable, even between sensors of the same type. However, these discrepancies are somewhat expected since the ADV and Smith meters sampled flows at higher elevations than that sensed by the video. For example, the minimum depth required for the in-situ gauges is on the order of 4 to 5 cm; and for optimal operation, the ADV sensor (positioned 5 cm above the sampling volume) must be fully immersed, thereby requiring depths of over 10 cm. The response times of the in-situ instrumentation appear to be somewhat slow, especially during uprush. Given that the in-situ instrumentation was out of the flow more often, coarsely sampled, and essentially excluded portions of the swash signal very near the bed, the video results, although simplified, appear sensible. One possible source of additional error is that obliquely incident swash motions will positively bias the cross-shore current estimates from the video. Measurements of the longshore trend of the swash edge suggest this error with respect to mean velocities was on the order of 10%. Longshore swash currents sampled with the ADV were less than 0.08 m/s.

	u_{up}	u_{down}	u^3	$u^3 u $	dur	m
Gleneden (235)						
Video	-0.94	0.85	0.07	0.12	6.4	0.33
Smith (4 cm)	-0.69	0.71	0.13	0.06	3.6	0.42
Smith (8 cm)	-0.71	0.64	0.04	0.02	3.4	0.43
Sandyduck (98)						
Video	-1.73	1.61	-0.28	-0.15	7.1	0.46
ADV (5-10 cm)	-0.83	0.89	-0.03	-0.01	4.5	0.38

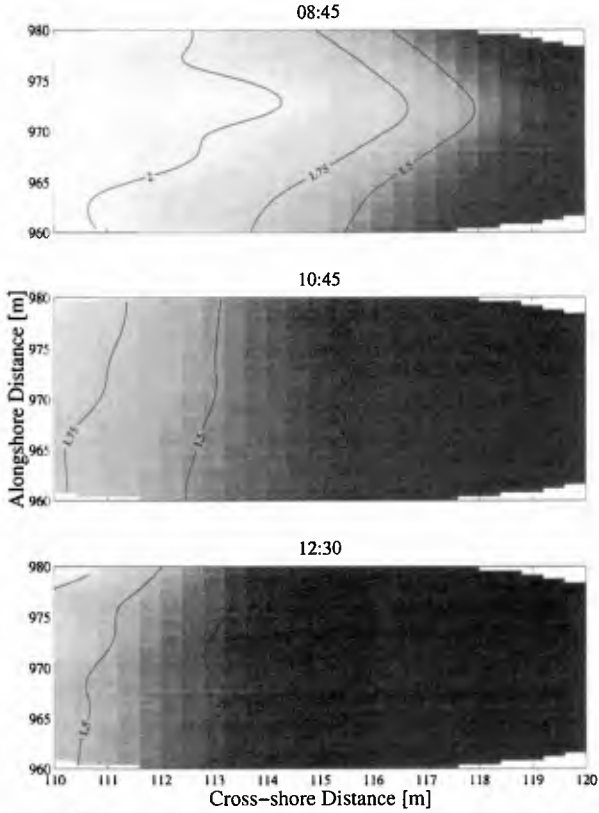
Table 1. Comparison of video-based and in-situ estimates of cross-shore swash velocity parameters. Symbols denote various swash moments, mean swash durations, and slope of the temporal velocity gradient.

Swash Velocity Characteristics

Unfortunately, no in-situ instrumentation was deployed during the Duck94 experiment, therefore, only video-based cross-shore current measurements were made. Over the approximately six-hour period of measurements, velocity magnitudes of up to 1.78 m/s were observed. The mean duration of a swash cycle at the approximate setup level was 3.9 s. Average initial uprush and final backwash speeds were essentially equivalent with magnitudes of 1.16 and 1.19 m/s respectively. However, shorter-term averages of the swash time series showed a tendency toward offshore-dominated flow prior to high tide and onshore-dominated flow during the falling tide. Also observed was an inequality between peak uprush and backwash velocities for individual swash events. Spatial gradients in the velocity structure tended to follow the trends in the mean velocities with positive gradients during the rising tide and negative gradients after high tide.

Foreshore Profile Change

Stereo-estimated foreshore surfaces on Oct 10 are shown in Figure 6. An optimal interpolation technique was used to fit the estimates to a constant grid surface, $h(x,y)$, with an even spacing of 40 cm between grid points. Temporal derivatives of the surfaces showed erosion rates of over 0.25 m³/hr with a maximum of 60 cm of erosion occurring in the center of the study area. Figure 7 shows the alongshore-averaged profile change rate as a function of cross-shore distance and time. A fairly constant loss of sediment is apparent proceeding in the landward direction with the rising tide. Of particular interest was the fact that the offshore wave conditions throughout the run were approximately equivalent, yet morphologic response was dramatically different before and after high tide.



October 10 1994

Figure 6: Stereo surfaces gridded and contoured following optimal interpolation analysis. The foreshore morphology changed from cusped at 0845 hours to plane by 1045 with more than 60 cm of erosion measured over the entire four-hour period.

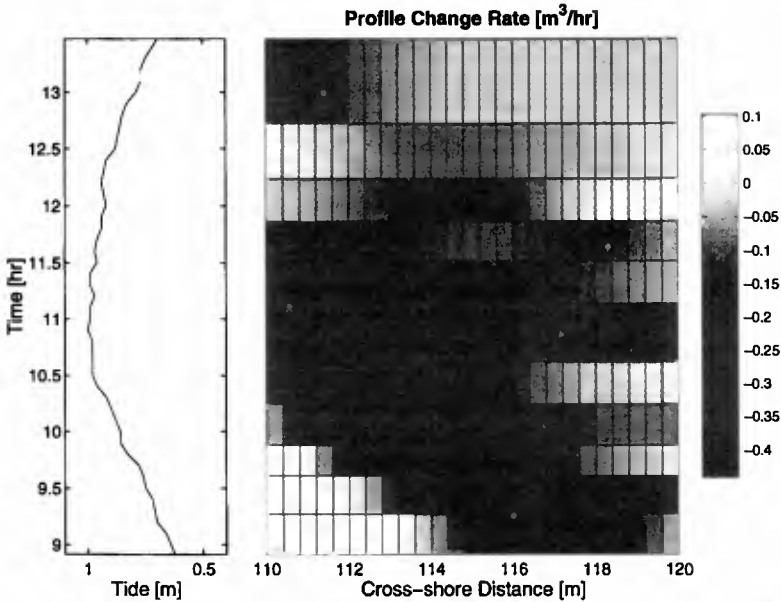


Figure 7: Alongshore-averaged profile change as a function of cross-shore distance and time.

Sediment Transport Model

A simple numerical model was developed and validated using the time histories of foreshore surface change in conjunction with video-based swash velocity measurements. Bagnold’s (1963; 1966) energetics-based, depth-integrated volume transport equation was adopted as the description of sediment dynamics for these data since it directly relates transport rates to instantaneous shear stresses derived from the local velocity field, $u(x)$. The form of the equation is given by:

$$q_t = \frac{\rho_w c_f}{(\rho_s - \rho_w)g} \left\{ \left(\frac{\epsilon_s (1 - \epsilon_b)}{\left(\frac{w}{\langle |u| \rangle} \right) - \tan \beta} \right) + \left(\frac{\epsilon_b}{\tan \phi - \tan \beta} \right) \right\} \langle u^3 \rangle \quad (1)$$

where q_t represents the time-averaged, cross-shore volumetric total sediment load transport per unit width per unit time, $\rho = 1.025 \text{ g/m}^3$ is the seawater density, $\rho_s = 2.65 \text{ g/m}^3$ is the sediment density, β is the beach gradient, ϕ is the friction angle of the sediment ($\tan(\phi) = 0.63$), w is the sediment fall velocity ($\sim 6 \text{ cm/s}$ assuming a mean grain diameter of 0.5 mm), and g is the gravitational acceleration. Angle brackets represent

time averaging and values for the friction, bedload, and suspended load efficiency factors, (c_b , ϵ_b , and ϵ_s , respectively) were defined following Bagnold (1966). This type of formulation has been previously applied to the swash zone (Hardisty et al. 1984; Hughes et al. 1997a; Masselink and Hughes in review) and serves as a good candidate model for these data using inputs of cross-shore current at a given cross-shore location and time varying beach slope.

Model results were compared to observations obtained using the stereo method by estimating profile change given spatial gradients in sediment transport predictions via the sediment continuity equation:

$$\frac{\partial h}{\partial t} = \frac{1}{1 - \nu} \frac{\partial q_s}{\partial x} \quad (2)$$

This relation assumes that no alongshore gradients in sediment transport contribute to profile change and ignores advection of sediment from the surf zone into the swash zone. The results, shown in Figure 8, indicate that the model was successful at describing the qualitative trends in profile evolution, however the magnitudes and positioning of observed sediment fluxes did not match the transport model predictions. For example, the erosion of the foreshore surface was observed to occur earlier than predicted. Also, a period of accretion was predicted after high tide (approximately 1230), while the measured profile remained stable.

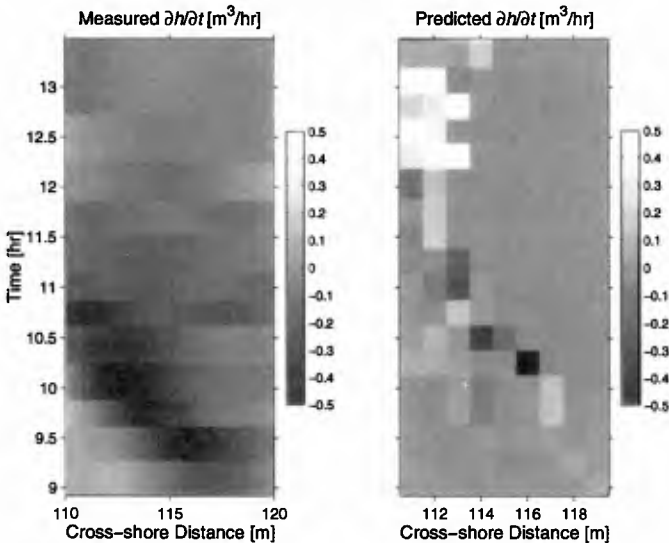


Figure 8: Measured (left panel) and predicted (right-panel) profile change as a function of cross-shore distance and time.

Discussion and Conclusions

Video-based methods were utilized to allow rapid and simultaneous measurement of swash zone hydrodynamic forcing and morphodynamic response. Although a small number of prior investigators have presented observations of swash zone sediment transport and cross-shore flow velocities, namely Hardisty et al. (1984), Hughes et al. (1997b), and Masselink and Hughes (in review), this study is distinguished by the large temporal and spatial coverage allowed by the video techniques. Another advantage of these methods is that velocity patterns associated with infragravity band wave motions are sampled. However, at present, alongshore currents cannot be directly estimated and extension of these methods to deeper surf zone flows is difficult.

An energetics-based sediment transport model (Bagnold 1963; Bagnold 1966) was validated using these data and was shown to be insufficient in predicting the magnitudes, and in some cases sign, of transport observed. Qualitative correlation between the model and observations during the first half of the measurement period suggests that swash flow velocity is an important parameter affecting foreshore sediment transport, however, the magnitude discrepancies indicate that other factors should be considered in future efforts. For example, the effects of water depth variations, infiltration, groundwater, and the influx of sediment from offshore, may well be responsible for a significant portion of the mismatch. One possibility for future adaptation of the model is through the use of variable efficiency coefficients during uprush and backwash as suggested by Masselink and Hughes (in review).

Acknowledgements

The authors thank the outstanding support personnel from the Scripps Institution of Oceanography and the US Army Corps of Engineers Field Research Facility for their assistance in the field data collections. We also appreciate the data contributions and insight of Mr. Jack Puleo and Dr. Reginald Beach. This work was funded by the Coastal Dynamics program at the Office of Naval Research, the US Geological Survey's Center for Coastal Geology, and from base program funding to the Naval Research Laboratory from ONR.

References

- Bagnold, R. A. (1963). "Mechanics of marine sedimentation." The Sea, M. N. Hill, ed., Wiley-Interscience, New York, 507-528.
- Bagnold, R. A. (1966). "An Approach to the Sediment Transport Problem from General Physics." 422-I, U.S. Geological Survey, 37.
- Beach, R. A., and Sternberg, R. W. (1992). "Suspended sediment transport in the surf zone: Response to incident wave and longshore current interaction." *Marine Geology*, 108(3-4), 275-294.
- Duncan, J. R. (1964). "The effects of water table and tide cycle on swash-backwash sediment distribution and beach profile development." *Marine Geology*, 2, 186-197.
- Guza, R. T., and Thornton, E. B. (1982). "Swash oscillations on a natural beach." *Journal of Geophysical Research*, 87(C1), 483-491.
- Hardisty, J., Collier, J., and Hamilton, D. (1984). "A calibration of the Bagnold beach equation." *Marine Geology*, 61(1), 95-101.
- Holland, K. T., and Holman, R. A. (1993). "The statistical distribution of swash maxima on natural beaches." *Journal of Geophysical Research*, 98(C6), 10,271-10,278.
- Holland, K. T., and Holman, R. A. (1997). "Video estimation of foreshore topography using trinocular stereo." *Journal of Coastal Research*, 13(1), 81-87.
- Holland, K. T., Raubenheimer, B., Guza, R. T., and Holman, R. A. (1995). "Runup kinematics on a natural beach." *Journal of Geophysical Research*, 100(C3), 4985-4993.
- Horn, D. P., and Mason, T. (1994). "Swash zone sediment transport modes." *Marine Geology*, 120(3-4), 309-325.
- Howd, P. A., and Holman, R. A. (1987). "A simple model of beach foreshore response to long period waves." *Marine Geology*, 78(1-2), 11-22.
- Hughes, M., Masselink, G., Hanslow, D., and Mitchell, D. (1997a). "Towards a better understanding of swash zone sediment transport." *Coastal Dynamics*, Plymouth, U.K., 804-823.
- Hughes, M. G., Masselink, G., and Brander, R. W. (1997b). "Flow velocity and sediment transport in the swash zone of a steep beach." *Marine Geology*, 138(1-2), 91-103.
- Masselink, G., and Hughes, M. (in review). "Field investigation of sediment transport in the swash zone." *Continental Shelf Research*.

- Osborne, P. D., and Rooker, G. A. (1997). "Surf zone and swash zone sediment dynamics on high energy beaches: West Auckland, New Zealand." *Coastal Dynamics*, Plymouth, UK, 814-823.
- Puleo, J. A., Beach, R. A., Holman, R. A., and Allen, J. S. (submitted). "Observations of swash zone sediment suspension and transport on a steep beach: Variations between the uprush and backwash and the importance of bore-generated turbulence." *Journal of Geophysical Research*.
- Raubenheimer, B., Guza, R. T., Elgar, S., and Kobayashi, N. (1995). "Swash on a gently sloping beach." *Journal of Geophysical Research*, 100(C5), 8751-8760.
- Sallenger, A. H., Jr., and Richmond, B. M. (1984). "High-frequency sediment-level oscillations in the swash zone." *Marine Geology*, 60, 155-164.
- Waddell, E. (1976). "Swash-groundwater-beach profile interactions." *Beach and Nearshore Sedimentation*, R. A. Davis, Jr. and R. L. Ethington, eds., SEPM, Tulsa, OK, 115-125.